8 OPTICAL ALIGNMENT AND CONTROL STRATEGY

8.1 Introduction

The segmented mirror aspect of GMT presents challenges both for optical fabrication, discussed in later chapters, and for maintaining alignment and phasing of the optics in operation. There are currently two approaches to building extremely large telescopes (ELTs), both using segmented primary mirrors. The small-segment approach uses a large number of mirrors each approximately 1 m in diameter. GMT relies on seven 8.4 m segments. Large segments have tighter alignment tolerances, but only in the lateral directions (lateral translation and rotation). The lateral tolerances for large segments are still loose in comparison with the resolution of their positioning actuators, so the wavefront accuracy will be limited by the wavefront measurement, not by the alignment of the segments. Axial tolerances (piston and tilt) are roughly independent of segment size, and for any segment size the axial tolerances are much tighter than lateral tolerances. In terms of linear displacements as opposed to angular displacements, large segments are favored: 1 micron of tilt across an 8 m segment is better than 1 micron of tilt across each of sixty-four 1 m segments.

The inclusion of a segmented secondary mirror in the optical design would at first seem to complicate the picture. In fact, it offers an opportunity to greatly simplify aligning and phasing of the telescope. The key feature is that the seven secondary mirror segments are conjugated one-to-one with the primary segments and can take care of the fine co-aligning and phasing of the subapertures. This greatly relaxes the position tolerances on the primary segments. The more agile secondary segments are also able to respond to disturbances much faster than the primary segments. The details are described in this chapter.

8.2 Overview

The GMT Telescope Control System (TCS) is responsible for pointing and tracking the structure, maintaining optical alignment and focus, and correcting wavefront errors due to distortion of the optical surfaces, the telescope structure and turbulence in the atmosphere. It consists of a hierarchical system of open and closed control loops operating in frequency regimes ranging from sub-hertz up to over a kilohertz. The TCS also provides interfaces to other subsystems of the telescope and observatory (instruments, archive, User Interface, enclosure, environmental controls, etc.).

GMT will implement three principal modes of control for the optics and structure: Active, Fast-tracking, and Adaptive. Active control is designed to correct slowly varying flexural and thermal distortions and produce images with negligible degradation for the best seeing-limited conditions when the wind-shake is low. Fast-tracking control and adaptive control involve fast control implemented with two different Gregorian secondary mirrors. Fast-tracking control will use a secondary with rigid fast tip/tilt segments, the Fast Steering Mirror (FSM) assembly, to stabilize image motion in the seven subapertures due to wind shake at mid-frequencies. Adaptive optics uses the Adaptive Secondary Mirror (ASM) to correct vibration and higher frequency wavefront errors originating in the atmosphere to produce diffraction-limited images at near- and mid-IR

wavelengths. It includes fast shape control and smooth slow tip/tilt control for each segment. The various flavors of GMT adaptive optics are described in Chapter 9.

The mount pointing and tracking system underlies all three modes. The TCS operates as the supervisor to synchronize signals between the control loops for the various modes and maintain stable operation.

Optical alignment and wavefront phasing is considerably more involved in a segmented mirror telescope than in a traditional monolithic mirror system. This problem has been addressed by Keck (Chanan et al. 1994 and subsequent papers) for primary mirrors with adjacent segments. The problem of coherently combining separated primary segments was addressed in the original MMT and now in the LBT for two 8.4 m segments. The strategy and hardware for phasing is described in Chapter 9.

The segmented secondary mirrors are the key to maintaining alignment and wavefront accuracy. The adaptive secondary mirror in particular, with shape resolution of a few nm and sub-ms response, makes it possible to align, control wavefront, and phase the seven sub-apertures to the diffraction limit in the near-IR. The GMT can reach an accuracy determined by fundamental limits of wavefront sensing, not by the optics.

8.3 Description

8.3.1 Control regimes

Pointing of the telescope relies on a library of standard algorithms that take as input the main axis encoder readings. Open-loop control of flexure and focus is based on observatory-generated look-up tables with the telescope elevation angle and secondary truss temperatures as inputs. The tables will be initialized during the commissioning phase of the telescope and periodically updated as required. Measurement of the pointing coefficients is done after the open-loop flexure terms are applied. The open-loop control reduces the magnitude of the corrections being driven by the closed loops, and shortens the set-up time required for alignment when slewing the telescope to a new object.

There are three distinct frequency regimes for the closed-loop control of the GMT:

- The *active optics* regime compensates for the residual gravitational and thermal deflections of the telescope structure and optics. Active optics control is typically restricted to frequencies below ~0.01 Hz.

- The *fast-tracking control* regime compensates for the mechanical eigenmodes of the telescope structure, including pointing. These eigenmodes are primarily excited by wind turbulence. Vibration control frequencies are typically in the range up to 10 Hz.

- The *adaptive optics* regime compensates for vibration and atmospheric disturbances of the wavefront, at frequencies up to 100 Hz.

8.3.2 Active controls

The active controls for GMT are an extension of the system developed for the 3.5 m, 6.5 m and 8.4 m borosilicate honeycomb mirrors, in particular the system used on the Magellan and LBT telescopes, to accommodate multiple subapertures. The purpose is to maintain collimation of the telescope optics to high precision, correct wavefront errors due to distortions of the optical surfaces, and maintain focus.

The control elements for the active optics system are the primary and secondary mirror segment position actuators (hexapods) and the primary mirror flotation actuators. The sensing elements of the active optics system are full-aperture Shack-Hartmann wavefront sensors deployed off-axis in the telescope focal surface (Section 8.4.1).

The individual primary mirror segments are installed in cells that incorporate flotation systems to minimize gravitational bending. If uncorrected, out-of-tolerance figure errors would develop as the telescope moves through its range in elevation, due to random force errors in the mirror supports. The thick cross sections of the segments resist high spatial frequency bending and only the low order bending modes (astigmatism, etc.) contribute significantly to the wavefront error in the natural seeing regime. These errors are sensed by the wavefront sensor and resolved into the natural bending modes of the mirror (Schechter et al. 2003). Corrective forces are then applied by the support actuators.

Temperature gradients in the non-zero CTE borosilicate glass also cause figure distortion of the primary mirror. The effect is most pronounced when the ambient temperature is rapidly varying, especially during the transition from day to nighttime observing. These typically induce bending in the radial modes where the mirror is inherently stiff, modes that require higher forces to correct than astigmatism, for example. A ventilation system is provided (Section 10.9) to promote rapid equilibration of the mirror with the air and reduce the magnitude of the corrective forces that must be applied.

Corrective forces up to approximately 10% of the gravity support force are used for active wavefront correction on the 6.5 m telescopes. Comparable forces will be required for GMT (Section 10.8).

A single wavefront sensor in the focal plane will not distinguish between wavefront errors originating on the primary mirror and those coming from the secondary mirror, fold mirrors on the instrument platform, or correctors. The active optics will correct the total wavefront from all surfaces at the position of the sensor in the field. Wavefront errors at other field points will be small as long as the spatial frequency of the errors is low. Multiple wavefront sensors in the field can resolve the ambiguity of errors originating on different surfaces and also sense focal length errors in the subapertures.

The second aspect of active control is correction for optical misalignment and de-focus. The seven primary mirror cells form a structural part of the 25 m diameter Optics Support Structure (OSS) of the GMT. Gravity and thermal deflections of the OSS are imparted to the cells and produce translations and tilts of the mirrors (Section 7.6.1). While the relative gravity displacements and tilts between segments for zenith to 30˚ elevation are remarkably small for a

structure this size, 140 microns RMS and 7.6 arcsec RMS respectively, they are still large compared to the alignment tolerances of Section 8.5.

Lateral displacement of the secondary mirror relative to the telescope optical axis due to flexure of the supporting truss moving from zenith to the minimum 30˚ elevation is Δy = -3.6 mm from Section 7.6.1. Piston motion relative to the primary mirror assembly will be 0.25 mm. These must also be sensed and corrected by the active system.

Displacements of the optics due to gravity will be fairly repeatable as a function of elevation angle and can be obtained to first order from look-up tables. The residuals will be sensed in the focal plane by the active optics sensors and corrected closed-loop.

The thermal distortion of the structure is less predictable. Over the full 35°C operating range of the telescope, the distance between primary mirror segments will change by 3.3 mm, and by 1.3 mm over the middle 90% range of temperatures, $+4°C < T < +17°C$. The temperature lapse rate on Las Campanas is in the range ±0.5 K/hr between the 20th and 90th percentile. Under these conditions the separation of the mirrors will change on average by about 0.05 mm/hr depending on the prior thermal history of the structure. The expansion will cause a de-stacking of the images from the subapertures. This will be sensed and removed by the fast tracking system (Section 8.3.3). The residual aberration will be sensed by the active optics wavefront sensor. A correction applied every 100 s would limit the effect on image size to θ_{80} < 0.002″.

Temperature also affects the separation between the primary mirror and secondary and hence the telescope focus. The truss supporting the secondary mirror will be made of steel or a combination of steel and carbon fiber reinforced plastic (CFRP). For the worst case all-steel truss the rate of change is in the range ±0.11 mm/hr for the same 20th to 90th percentile conditions. This corresponds to Gregorian focus changes of ±14 mm/hr, or up to 1.5 arcsec/hr in image size. Temperature sensors on the truss legs provide feedback to determine length change and command compensating motions by the secondary focus actuator. On Magellan this is accomplished by measuring the resistance change of an electrically insulated, thermally contacted platinum wire bonded along the full length of one leg and applying focus corrections more-or-less continuously from a look-up table. The same system will be employed on GMT. The residual focus errors will be sensed by the active optics wavefront sensor. In order to maintain piston accuracy of 1-2 microns, corrections need to be applied every 30-60 seconds. Wavefront measurements could be made less frequently because the trend will be predictable for periods of several minutes.

The active optics wavefront sensors cannot easily distinguish between position errors of the primary and secondary mirror segments. GMT is unique among segmented mirror telescopes in that misalignment of the individual primary segments can be corrected by compensating motions of the conjugated secondary segments and vice versa. This is true for both the wide-field seeing-limited regime and the narrow-field diffraction-limited regime for primary segment position errors up to ~3.5 mm as described in Section 8.5. Errors of this magnitude might arise from thermal expansion of the primary mirror support structure.

While in principle the full range of primary segment misalignment can be corrected entirely by moving the secondary segments, with no significant loss in image quality over the full 20 arcmin

field, our preferred strategy is to control the primary segment positions to approximately ±100 microns, comparable to the gravity deflections through the full range of elevation motion, by periodic adjustments to the hexapods that support each primary segment. This is well within the expected accuracy of the hexapod actuators. Deflection of the truss will be compensated by moving the entire secondary assembly with the main secondary hexapod. Any remaining residual errors will be corrected by fine motions of the individual secondary segment hexapods.

The active optics wavefront sensor must integrate for 30 seconds or longer in order to average out the high-frequency wavefront errors induced by atmospheric seeing. On the Magellan telescopes only a fraction, typically 30%, of the sensed error is applied in each 30 second cycle as active corrections to the optics and structure. This effectively increases the averaging time. The fraction is set in software and can be changed by the telescope operator depending on conditions, but is normally left at its nominal value. Fortunately, this long control interval is appropriate for the low bandwidth errors which the active optics system is intended to compensate. Segment collimation and figure control is typically carried out through the lowest 20 or 30 mechanical modes of each primary mirror segment. Field aberrations at the location of the sensor probe are removed before corrections are applied to the optical system (Schechter 2003).

8.3.3 Fast-tracking Control Mode

The lowest order vibration control (beyond the main axis drives) is control of the tip/tilt secondary mirror, or in the case of GMT, the seven-segment Fast-steering Secondary Mirror described in Section 11.4. Higher-order modal control will be made using the Adaptive Secondary Mirror, Section 11.3. One of the important features of the GMT is that the very stiff mechanical structure and primary mirror segments avoid the requirement for vibration control at frequencies >10 Hz for seeing-limited observations. The sensing elements for the fast-tracking control system are the main axis encoders and a deployable offset guide camera which produces seven images, one for each mirror segment. In order to maintain optical and mechanical simplicity, the guide camera will typically be deployed outside the isoplanatic patch. The field of view of a seeing-limited instrument may be larger than the isoplanatic patch as well. This leads to a compromise situation in which segment tip-tilt errors which arise in the telescope will be corrected by the fast-tracking control system, but tip-tilt errors which arise in the atmosphere may not be improved or may even be made somewhat worse. There is likely to be a clear benefit to using fast-tracking tip-tilt control under high-wind conditions, but otherwise the image quality is likely to be no worse or even slightly better if the system is turned off. This compromise is no different from the situation which arises to a lesser or greater extent with all of the current generation of 8 m class telescopes.

Accumulated pointing corrections in the fast-tracking control system will be off-loaded to the mount at low bandwidth to reduce the stroke requirements of the fine motion actuators.

8.3.4 Adaptive Control

The control elements for the adaptive optics system are the actuators on the deformable secondary mirror segments, and the position controlled legs of each secondary segment hexapod. In order to achieve the required positioning accuracy combined with adequate stroke, the

secondary segment hexapod actuators may require separate fine and coarse adjustment mechanisms. The sensing elements are (i) optical Shack-Hartmann sensors for the laser guide stars and natural guide stars, (ii) near-infrared natural guide tip-tilt and (iii) phase sensors. These all are in separate packages which operate within the isoplanatic patch by means of dichroic mirrors. There may also be accelerometers on the secondary sub-frame supporting the seven segments, and if necessary on the individual seven primary segments (see Section 9.4).

When adaptive optics control is in use, the functioning of the active optics system will be modified. Tip-tilt errors accumulated over the reference gap of each adaptive secondary segment will be continuously off-loaded to the fine-positioning actuators in the secondary segment hexapod legs, which will allow for smooth (10 nm) motion up to ~100 microns. Only when these legs have accumulated an adjustment on the order of 50 μm from the nominal position will the error be off-loaded to the coarse-adjustment actuators in the secondary hexapod, when there will be a discontinuous step. In this way the accompanying ~1 second breaks in adaptive control will be no more frequent than every few minutes. The main telescope drives will be used to off-load the long-term global tip-tilt correction. The active optics wavefront sensors will still be deployed, in order to set up on a target field or to maintain the telescope configuration when adaptive control is interrupted.

Two additional systems will be useful in configuring the telescope and checking that the control loops are operating correctly. The first of these is a secondary calibration light source which can be inserted by remote control at the nominal prime focus of the telescope. It is described in Section 11.3.8. The second system is the primary mirror edge sensors, described in Section 8.4.2 below.

In the seeing-limited regime, observing the secondary calibration light source with the active-optics wavefront sensor will allow the secondary mirror segments to be aligned relative to one another, and the figure of each segment and of the overall secondary to be verified. Then the primary mirror segments can be aligned by observing starlight with the active-optics wavefront sensors. Once the reference position of the primary mirror segments has been established, the edge sensors should provide long-term stability (until a segment is replaced with a freshly aluminized one, for example) of the primary mirror alignment within a few microns. However, it is important to note that information from the active optics wavefront sensor alone is sufficient to maintain alignment of the telescope optics during the night.

In the diffraction-limited regime, the phasing of the seven secondary segments alone will be established by the secondary calibration light source with the AO phasing camera. The phasing of the wavefront across the full telescope aperture will use this camera continuously viewing starlight in the near infrared. The primary mirror edge sensors will provide additional high-speed inputs to the adaptive optics phasing control loop.

8.3.5   Summary

It is important to ask how this control scheme differs from the experience of the various groups working on the current generation of 8 m class telescopes. In the first instance the lowest resonant frequencies of the mount will be somewhat lower than the best examples among current telescopes (~4 Hz compared to ~8 Hz), but still comparable to some existing telescopes which

operate very successfully. Balancing the lower resonant frequency are the larger size and mass of the main telescope structure, which act as a stronger low-pass filter on the spectrum of wind perturbations. The relatively small wind cross-section of the secondary assembly is also helpful in this regard. Dynamical response analysis of the GMT structure indicates that the dominant effect of wind will be vibration at ~8 Hz, but that this will be significant only in high wind. Even without fast-tracking control, seeing-limited performance would meet the standards of the current generation of large telescopes, some of which require additional correction for wind-shake in order to achieve adequate seeing-limited performance. The relatively small (1.06 m diameter) GMT secondary mirror segments make fast tip-tilt correction at the Fast-steering Secondary Mirror a viable option. The servo motions of the adaptive secondary required to correct the full wavefront for vibration induced aberrations also appear tractable, as we discuss in Chapters 9 and 11.   Both the lightweight fast-steering mirror and the adaptive secondary can virtually eliminate image motion due to wind, within the accuracy of measurement.

8.4   Sensors

8.4.1   Active Wavefront Sensor

The Shack-Hartmann Active-Optics Wavefront Sensor (AWS) provides feedback to the active correction system for maintaining optical alignment, focus, and mirror figure. The active optics system corrects only the slowly varying distortions of the telescope that occur on a time scale that is long compared to the time required to integrate out seeing effects in the wavefront sensors, 30 seconds or more.   Multiple sensor probes will be mounted on separate stages in the Instrument Platform Guider Assembly (IPGA) below the top plate of the platform. The number of probes required will be determined in the next phase. Magellan has two wavefront probes in its guide assemblies but only operates with one at any time.

During operation the probes will be moved around in the field of view to pick up reference stars for the wavefront measurement. In general the probes will be deployed in an annulus outside of the field of view of the science instrument but they will have the capability to reach into the center of the field for on-axis calibration.   They will share this patrol area with fast sensors for rapid guiding and co-alignment of the seven subapertures. The adaptive optics system will have its own separate set of wavefront sensors above the IP for measuring atmospheric wavefront errors (Chapter 9).

The components of the AWS consist of a pick-off mirror located above the telescope focal plane, an aperture for sky background suppression, an achromatic collimator lens, the lenslet array, and a cooled CCD detector, Figure 8-1. A calibration source for the sensor will be provided by a pinhole light source and beam splitter (not shown) to inject the calibration beam. In the final design a red filter may be included to limit the bandpass. Table 8-1 lists basic specifications for the proposed design. A full description is given by Johns (2005b).
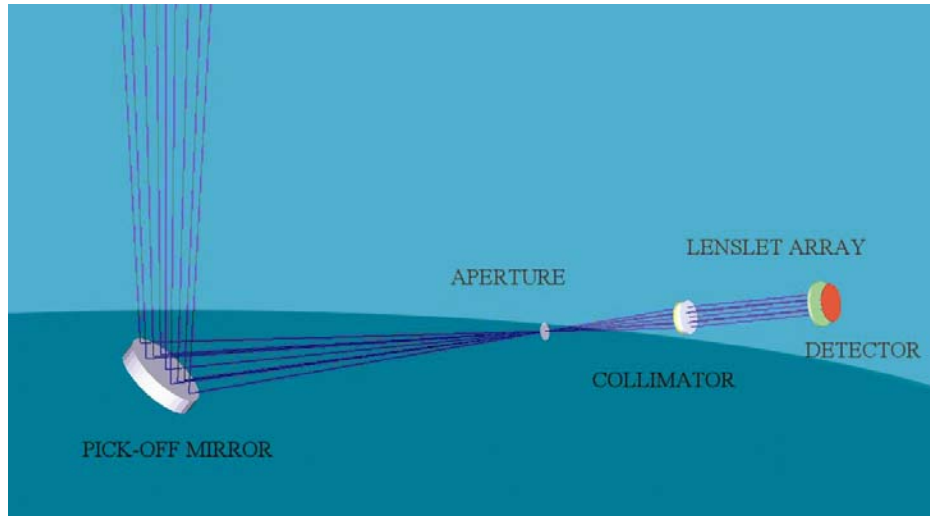
Figure 8-1. Active-optics Wavefront Sensor (AWS).

Table 8-1. AWS Components	
Pick-off mirror	36 mm x 48 mm elliptical flat
Pin hole	10 mm (9.8 arcseconds)
Collimator	Achromat, 90 mm f.l.
Lenslet array	48 x 48 sq. grid, 0.3 mm pitch, 5.8 mm f.l.
CCD	E2V CCD47-20BT (AIMO), 1024 x 1024, backside thinned.

The collimator lens forms an image of the primary mirror entrance pupil on the lenslet array. The focal length of the collimator is chosen such that the image underfills the array. In order to keep the image centered on the array the sensor probe will be articulated to stay pointed at the pupil as the probe moves around the focal plane. The lenslet pitch corresponds to a sampling distance of 687 mm on the surface of the primary mirror which provides adequate sampling for the required number of modes and ensures the availability of sufficiently bright reference stars over the whole sky.

Figure 8-2 shows the pattern of Shack-Hartmann spots on the CCD. Spot separation is 4.8" which is adequate for centroiding under most seeing conditions. Software is required for (1) finding and centroiding the spots, (2) fitting a set of basis functions to the centroid positions, (3) separating out the terms for alignment and segment figure correction, (4) commanding motions of the active alignment and segment support subsystems, and (5) recording and displaying the results. The software developed for the single-mirror Magellan and MMT telescopes and LBT will be adapted for GMT.
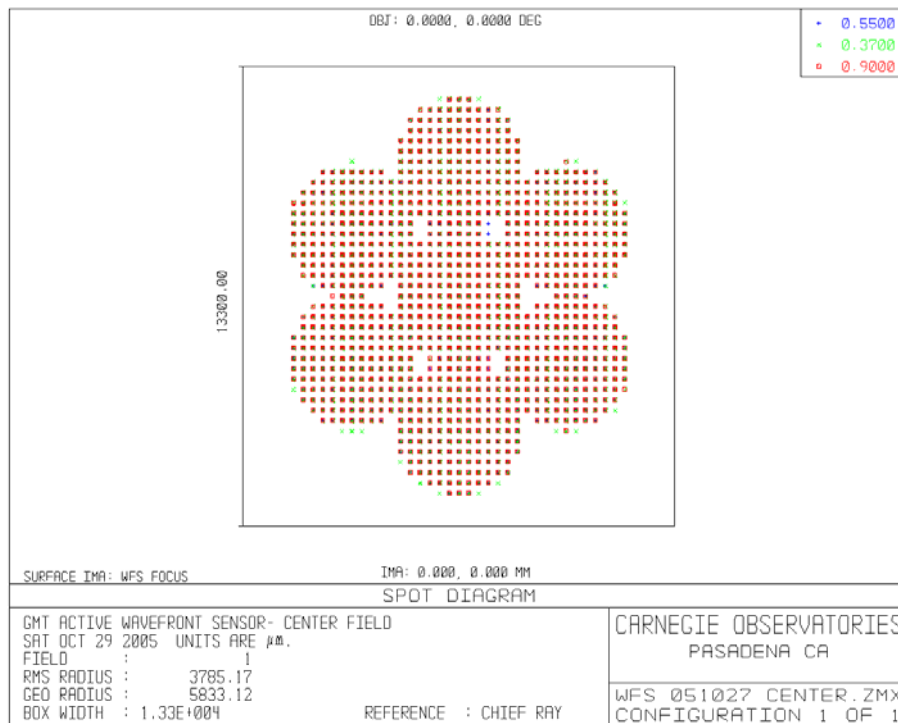
Figure 8-2. Shack-Hartmann spots for the narrow field, on-axis case. Box shows the CCD array size. Spot separation is 4.8 arcsecs.

8.4.2 Primary Mirror Edge Sensors

The adaptive optics segment piston sensor uses an off-axis guide star to produce an accurate measurement of the relative phase between mirror segments every minute or so. The segment piston sensor concept is discussed in Chapter 9. Between measurements the primary mirror edge sensors will provide real-time (~200 Hz) measurements of the change in relative position of the primary mirror segments. The goal is to measure the primary segment positions with an accuracy of 30 nm. The edge sensors should also be stable to within a few microns long-term (weeks) and can be used to check the coarse adjustment of the primary mirror hardpoints.

The GMT edge sensor concept uses two optical beams to measure the relative tilt and displacement between adjacent points on two mirror segments. The separation between mirror segments is significant (~500 mm at the location of the edge sensors) so an optical solution is in some ways more convenient than a mechanical sensor which would have to physically bridge the gap.

An optical layout of an edge sensor is shown in Figure 8-3. There are two optically similar units, a projector on one mirror segment (left) and a viewer on the other mirror segment (right). A light source on the projector is used to project an array of spots, in order to produce a more accurate measurement than a single pinhole. Two beamsplitters, one in the projector and one in the viewer, are used to produce two separate optical paths through the system. The lower optical path is collimated while the upper path produces an intermediate image of the spot array midway

between the two segments. A collimating lens in the projector, and a focusing lens in the viewer relay the image through the collimated path from the spot array in the projector to a TV camera in the viewer. Two additional lenses in the imaging path focus and re-collimate the intermediate image.
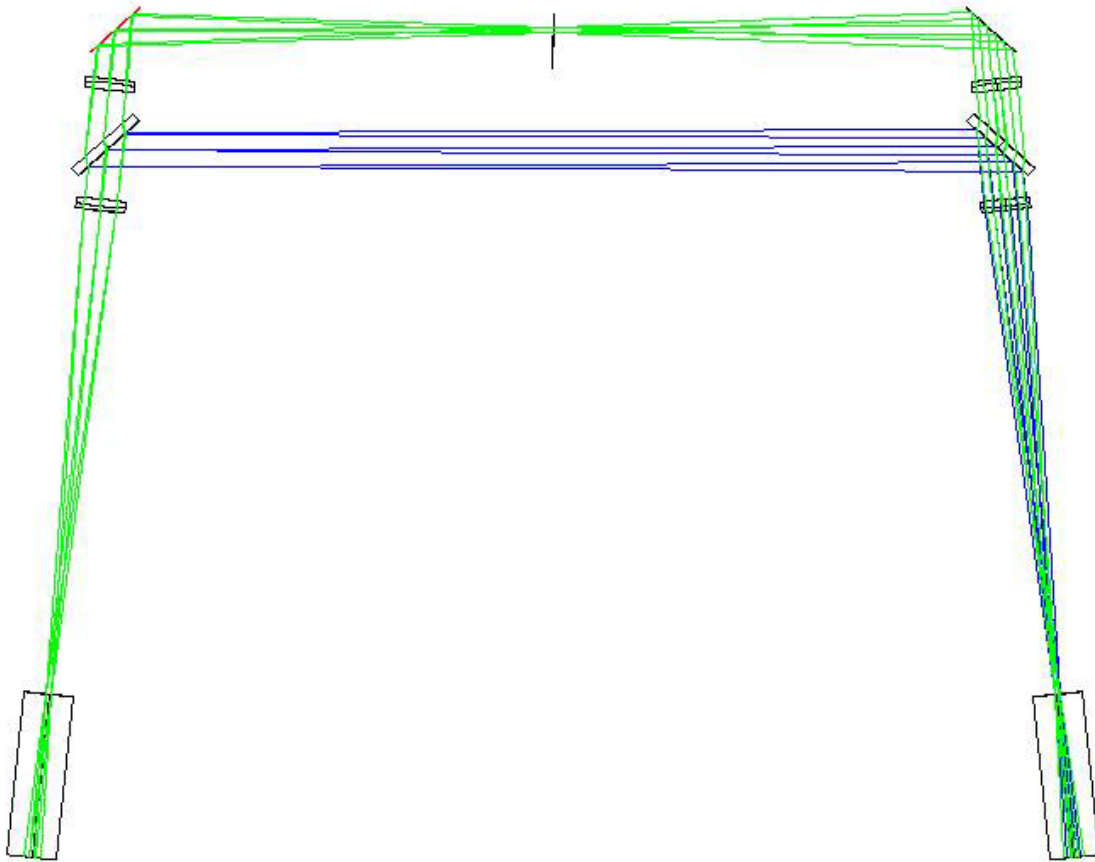

Figure 8-3. Optical layout of a GMT primary mirror edge sensor. The light source is shown schematically on the left and the TV camera on the right. A beam splitter in each leg is used to produce separate optical paths for the lower collimated beam (which measures tilt) and the upper focused beam (which measures displacement)

All four lenses in the system are stock achromats (in the diagram they are 30 mm diameter x 300 mm FL). The spot array is re-imaged onto the TV camera 1:1. A small offset in the angle of one of the diagonal mirrors is used to separate the two sets of spots (collimated and intermediate image) on the detector. The X and Y positions of the spots through the collimated path provide a measure of the tip and tilt angles between the two segments along axes perpendicular to the collimated optical path. The X and Y positions of the spots through the path with an intermediate image provide a measure of the displacement between the two segments at the position of the intermediate image.

The optical system which relays the images is relatively slow and the image quality is quite good. If the spots are illuminated with a yellow LED (where the color correction of the stock lenses is best) the images should be diffraction-limited, with a FWHM through either optical path of about 10 μm. A commercial CCD camera with fairly small (<10 μm) pixels and good

dynamic range should have no difficulty producing average position measurements for the spot arrays which are much more accurate than 1 micron. In principle, with a S/N ratio of 100:1 and 100 spots, the RMS position error should be only 4 nm. The "seeing" along the relatively short optical path will be much less than 1 arcsec, but 0.01 arcsec (FWHM) of seeing corresponds to an RMS position error of 6 nm. An immediate goal for the next phase of the GMT project is to build a prototype of the optical edge-sensor in order to investigate whether such high precision can be achieved in practice.

At f/10 the separation between the projector and viewer will have to be maintained to better than 100 μm in order to keep the images in good focus. A remote focus adjustment for one of the lenses in the intermediate image path will be required, and if the thermal change in the focal length of the lenses is strong enough, possibly in the collimated path as well. In order to collimate the system and zero the position of the spot array on the detector, the angles of two of the diagonal mirrors will need to be manually adjusted when installing a projector and viewer pair. Other adjustments in the system should be permanent and made on an optical bench when each projector or viewer is assembled.

The complete edge-sensor system is highly redundant, consisting of 24 tilt+displacement sensors, two between each of the 6 adjacent off-axis segments, and two between each off-axis segment and the center segment. The two separate sensors between each pair of adjacent mirror segments are widely separated (by about 3 m), providing additional coupling between tilts and displacements in the numerical solution of the complete system. For the Keck edge sensor system, the RMS surface error for the primary mirror is 4.5 times the RMS displacement error for a single sensor. A numerical model of the GMT edge-sensor system is also a near-term goal of the design study, but it seems unlikely that the multiplier will be much larger than it is for Keck.

Each off-axis mirror cell will be equipped with an electronics package capable of monitoring the output of 4 edge sensors. The first mirror segment has been cast with a series of raised bosses around its perimeter for mounting the edge sensors. A schematic cross-section of an edge sensor mounted on a primary mirror segment is shown in Figure 8-4. Note that there is an opaque seal around the periphery of each mirror segment. Since there will also be internal baffles in the light source for the spot array, as well as along the optical path of the projector and the viewer, there should be relatively little scattered light escaping from the edge sensors. This will be an additional area to be studied with the edge sensor prototype. The primary mirror cells and cell connector frame have been designed to allow personnel access to the edge sensor mounting points for installation, maintenance and adjustment.

The secondary mirror assembly is much more compact and it should be possible to make it considerably more stable than the primary. It is not yet clear whether an additional set of edge sensors will be required in order to monitor the relative positions of the secondary mirror segments over short time scales. The secondary mirror segments are much closer together (the gap is about 50 mm) and a more conventional mechanical or electrical sensor system is likely to be preferred if it becomes necessary to implement a secondary mirror edge sensor system.
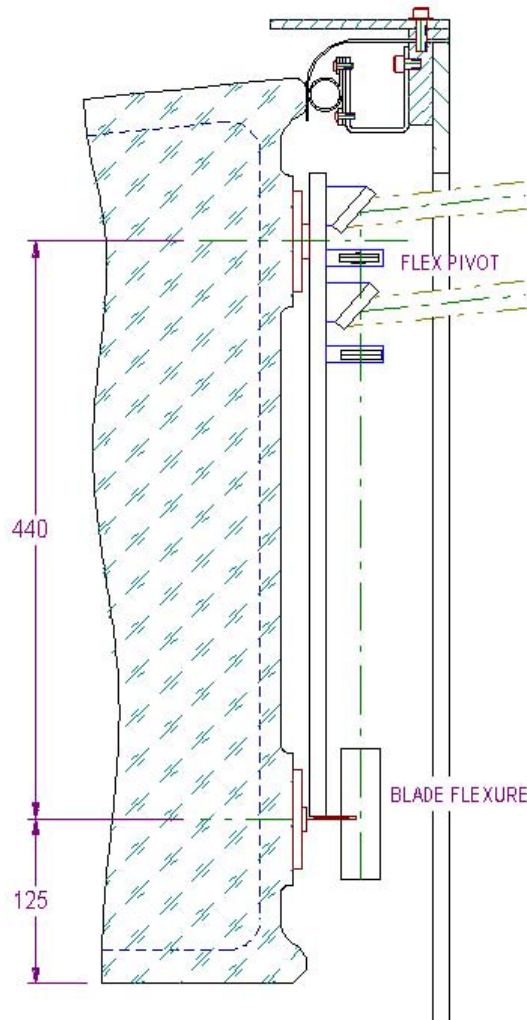
Figure 8-4. Schematic cross-section of an edge sensor mounted on a primary mirror segment.

8.5 Active Control of Optical Misalignment

8.5.1 Compensation using Secondary Segment Motions

The degree to which alignment errors originating with the primary mirror can be corrected by moving the secondary mirror segments has been investigated using an optical model of the telescope with segmented primary and secondary mirrors. Two cases have been considered: (1) correction of on-axis images for high-Strehl (AO) operation and (2) wide-field correction over the full 24′ diameter field of view of GMT.

The correction of primary mirror misalignments using motions of the corresponding secondary segment was modeled using the subaperture of the telescope defined by off-axis primary mirror segment P1 and its corresponding secondary segment S4, Figure 8-5. The results apply to the other subapertures through a simple rotation of coordinates.
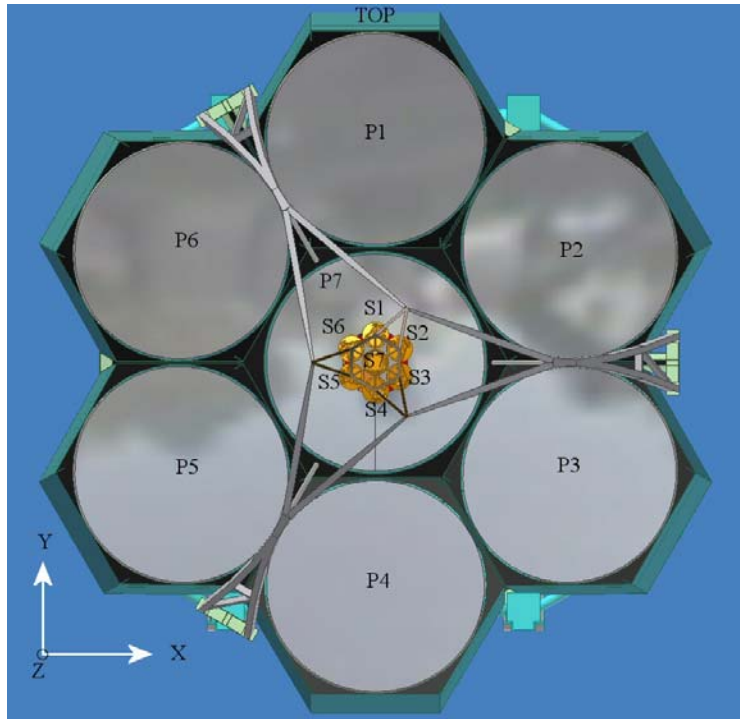
Figure 8-5. Segmented mirror labeling.

The off-axis mirrors are modeled as segments of the on-axis parent Gregorian surface which has its vertex on the optical axis of the telescope. The coordinates (x, y, z) and the tilts ($\theta_x, \theta_y, \theta_z$) are referenced to the coordinate system centered on the vertex of the parent. A transformation must be applied to get displacements and tilts local to the segment. Xtilt, Ytilt, and Ztilt refer to tilts about the center of the primary segment and are combinations of tilts and translations in parent coordinates. Local motions of the secondary segment in addition to the displacements in parent coordinates are provided in the output tables. The displacements in the local coordinate system are useful in determining actuator range.

Perturbations were applied to segment P1 and the system was re-optimized for best performance allowing selected position and tilt parameters of segment S4 to vary. In several cases different combinations of secondary segment parameters were allowed to vary for the same initial perturbation of the primary in order to investigate the correction possible with different combinations.

RMS spot sizes and wavefront errors are calculated for the subaperture with respect to the chief ray for the center mirror at the standard wavelength of 500 nm. The merit function used for the optimization was a weighted combination of RMS spot size and optical path difference. Different weighting factors can produce slightly different results but they will not change the overall conclusions.

The location of the focal plane relative to the center mirror and field curvature are not allowed to vary from the baseline design. The RMS spot size includes both tilt and higher order aberrations and hence provides a measure of image blur with respect to the chief ray.

The displacements and tilts modeled for the primary segment were chosen to be of comparable magnitude to the uncorrected displacements due to gravity sag and well within the positioning accuracy of the mirror support system. The results can be linearly scaled up or down for other values. The displacement values for the initial runs are typically 100 microns translation and 0.001° tilt. The precision that is currently thought to be achievable using the evolved hexapod mechanisms developed for successive generations of SOML mirrors, including MMT, Magellan, and LBT, is a factor of 10-50 better than this.

The spot sizes and optical path differences from the unperturbed parent optical design are included in the results. For the narrow-field case with no corrector these are essentially zero. For the wide-field case the corrector adds to the aberrations across the full field. The plate scale of GMT is 1.02 arcsec/mm.

8.5.2   On-axis Correction

The model for investigating on-axis correction is based on the two-mirror parent design of GMT without corrector or ADC. This is the appropriate case for narrow-field applications such as high-Strehl adaptive optics.

The results are shown in Table 8-2 for an assumed set of primary mirror segment displacements and tilts. The first column gives the perturbation that was applied to the primary mirror segment. Columns 2-6 give the displacements and tilts of the secondary segment after optimization. Columns 7, 8, and 9 give the RMS spot diameter, peak-valley wavefront error, and RMS wavefront error respectively.

In all cases the corrected image sizes are less than 5.2 microns (0.005 arcsec) RMS radius and peak-valley wavefront errors less than 0.4 wave at 500 nm for the assumed perturbations. In general most of the residual wavefront error is in low order modes that is correctable well below these already small values with active or adaptive figure control on the primary or secondary mirrors.

Table 8-2. On-axis correction of optical misalignments. (Δx, Δy, Δz) and (θx, θy) are displacements and rotations respectively in the parent coordinate system. Xtilt, Ytilt, and Ztilt are rotations of the segment about its mechanical center parallel to the parent x-, y-, and z-axes. Values in italics were held fixed.

On-axis correction of primary mirror segment misalignment with secondary mirror segment motions.								
M1 Perturbation	M2 global displacements			M2 Tilts		Spot RMS radius wrt chief ray	Wavefront error waves (λ = 500nm)	
	Δx	Δy	Δz	θx	θy			
(microns,arcsec)	microns	microns	microns	arcsec	arcsec	microns	P-V	RMS
Unperturbed	*0*	*0*	*0*	*0.00*	*0.00*	0.0	0.005	0.000
Δx = 100 μm	109.6	*0.0*	*0.0*	*0.00*	-0.87	0.1	0.003	0.001
Δy = 100 μm	*0.0*	109.7	*0.0*	0.87	*0.00*	0.0	0.001	0.000
Δz = 100 μm	*0.0*	-3.5	100.0	-0.18	*0.00*	0.6	0.032	0.007
θx = 3.6"	*0.0*	*0.0*	*0.0*	-28.30	*0.00*	5.2	0.373	0.096
θx = 3.6"	*0.0*	9.0	*0.0*	-28.30	*0.00*	1.3	0.057	0.013
θy = 3.6"	*0.0*	*0.0*	*0.0*	*0.00*	-28.30	1.0	0.222	0.012
Xtilt=3.6"	*0.0*	-8.8	-152.0	-27.90	*0.00*	0.9	0.050	0.011
Ytilt=3.6"	14.4	*0.0*	0.0	*0.00*	-28.20	0.2	0.013	0.003
Ztilt = 3.6"	166.6	*0.0*	*0.0*	*0.00*	-1.32	0.0	0.000	0.000
Δy = 3000 μm	*0.0*	3293.0	*0.0*	26.35	*0.00*	2.8	0.169	0.040

8.5.3 Wide-field Correction

The optical model for investigating the correction of primary mirror segment misalignment over a wide-field with the secondary mirror segments includes a simple (monochromatic) BK7 doublet corrector optimized for field diameters up to 24′ at λ = 500 nm rather than the 20′ achromatic wavefront corrector/ADC described in Chapter 6. This was done to avoid the non-azimuthally symmetric PSF variations that are not relevant for this analysis. Figure 8-6 shows the modeled corrector.
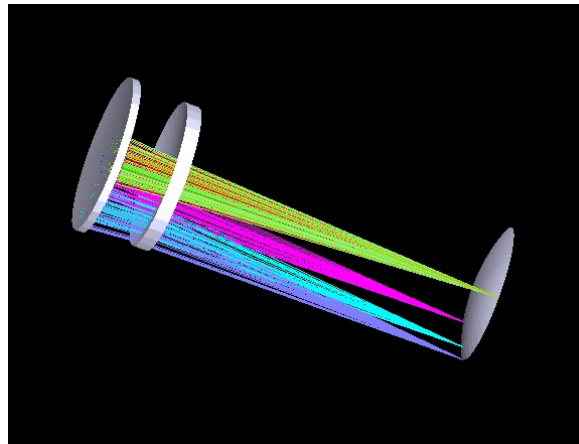

Figure 8-6. Simple 24′ wide-field corrector.

The results are shown in Table 8-3 for an assumed set of primary mirror segment displacements and tilts. Column 1 gives the perturbation applied to the primary mirror segment. Columns 2-6 give the displacements and tilts of the secondary segment after optimization. Columns 7-10 give the RMS spot radius for field angles of 0′, 6′, 10′ and 12′ respectively. Columns 11 and 12 give the peak-valley and RMS wavefront error on axis.

Table 8-3. Wide-field correction of misalignments. (Δx, Δy, Δz) and (θx, θy) are displacements and rotations respectively in the parent coordinate system. Xtilt, Ytilt, and Ztilt are rotations of the segment about its mechanical center parallel to the parent x-, y-, and z-axes. Values in italics were held fixed. RMS spot radii are RMS values calculated on the ±x- and ±y-axes in the focal plane for each field radius.

Correction of primary mirror misalignments out to a field radius of 12 arcminutes with the Corrector/ADC using secondary mirror segment motions.											
M1 Perturbation	M2 Global Displacements			M2 Tilts		RMS radius wrt chief ray (microns)				Wavefront error	
	Δx	Δy	Δz	θx	θy	Field radius				waves (λ = 500nm)	
microns, arcsec.	microns	microns	microns	arcsec	arcsec	0'	6'	10'	12'	P-V	RMS
Unperturbed	*0.0*	*0.0*	*0.0*	*0.0*	*0.0*	12.2	39.3	28.7	51.1	0.749	0.151
Δx = 100 μm	109.4	*0.0*	*0.0*	*0.0*	-0.9	12.2	39.6	28.7	51.1	0.750	0.152
Δy = 100 μm	*0.0*	95.6	*0.0*	0.2	*0.0*	19.6	37.4	30.0	53.9	1.093	0.260
Δz = 100 μm	*0.0*	*0.0*	100.0	*0.0*	*0.0*	8.7	42.9	32.4	47.1	0.952	0.096
θx = 3.6"	*0.0*	*0.0*	*0.0*	-28.3	*0.0*	17.8	23.7	57.1	108.6	1.133	0.261
θy = 3.6"	*0.0*	*0.0*	*0.0*	*0.0*	-28.3	12.3	42.4	38.4	59.7	0.718	0.154
Xtilt=3.6"	*0.0*	-8.4	-152.0	-27.9	*0.0*	16.5	23.9	59.8	111.9	1.133	0.256
Ytilt=3.6"	5.3	*0.0*	*0.0*	*0.0*	-27.8	12.4	42.3	38.3	59.7	0.746	0.156
Ztilt=3.6"	166.4	*0.0*	*0.0*	*0.0*	-1.3	12.2	39.5	28.7	51	0.751	0.152
Δy = 3000 μm	*0.0*	3278.0	0.0	*25.6*	0.0	19.9	46.8	36.1	31.4	1.265	0.298

The maximum residual uncorrected misalignment error over the specified 20′ field is less than 53 microns (0.054 arcsec) RMS radius after subtracting the contribution from the basic optical design in quadrature for the assumed primary mirror perturbations.

Averaging the field radius terms in Table 8-3 in quadrature gives the error budget for primary mirror segment misalignment for the position tolerances shown in Table 8-4. This is an approximate treatment that does not fully account for the weighting of errors by area or optimization of the secondary segment compensators that could further reduce the sums.

Table 8-4. Error budget for misalignment of the primary mirror segments. Wide-field (Case 2) optimization.

Error budget for primary mirror segment misalignments after correction with the secondary mirror segments.						
M1 Perturbation	Tolerance	Units	20 arcmin FOV		24 arcmin FOV	
			RMS radius microns	80%ee microns	RMS radius microns	80%ee microns
Δx	100.0	microns	2.8	7.1	2.4	6.2
Δy	100.0	microns	7.4	18.8	10.7	27.2
Δz	100.0	microns	12.2	31.1	3.7	9.5
Xtilt	3.6	arcsecs	25.2	64.0	54.3	138.0
Ytilt	3.6	arcsecs	17.3	43.8	21.5	54.6
Ztilt	3.6	arcsecs	2.3	5.8	1.2	3.0
		RSS (microns):	33.9	86.1	59.6	151.4
		RSS (arcsec):	0.034	**0.088**	0.061	**0.154**

8.5.4   Secondary Mirror Segment Alignment Tolerances

The sensitivity of the GMT optical system to misalignments of the secondary mirror segments in the seeing-limited (active optics) mode was analyzed by applying selective displacements and tilts to segment S4 and recording the displacement and RMS spot size of the image in the focal plane. To first order the aberrations are independent of field position and only an on-axis point source is modeled. The results scale linearly and can be used to obtain the image displacement and spot size for other values of segment displacement and/or tilt.

The applied displacements and tilts are relative to the center of the front surface of the segment:

- Δx is a displacement parallel to the surface and parallel to the global x axis.

- Δyz is a displacement parallel to the surface in the y-z plane.

- Piston is a displacement parallel to the surface normal at the center of the front face.

- Xtilt is a local tilt about an axis through the center point parallel to the global x-axis.

- Ytilt is a local tilt about an axis through the center point parallel to the global y-axis.

- Ztilt is a rotation about the segment center parallel to the global z-axis.

Table 8-5 gives specifications and goals for secondary mirror segment displacement and tilt tolerances derived from the sensitivity calculations and the error budget allocation for this source of error. The relative amounts may be re-balanced as required by the mechanical design as long as the RSS value for 80% enclosed energy does not exceed the allocation. Feedback for determining these motions will be derived from the active wavefront sensors in the focal plane.

Table 8-5. Secondary mirror segment alignment tolerances.

Secondary Mirror Segment Position Tolerances									
		Sensitivity		Specification			Goal		
Parameter	units	displ	RMS spot microns	Tolerance	RMS spot microns	80% ee microns	Tolerance	RMS spot microns	80% ee microns
Δx	microns	10	114.8	2.0	23.0	58.3	1.0	11.5	29.2
Δyz	microns	10	112.2	2.0	22.4	57.0	1.0	11.2	28.5
Piston	microns	10	25.4	4.0	10.2	25.8	1.0	2.5	6.5
Xtilt	arcsec	0.36	88.9	0.11	26.7	67.7	0.07	17.8	45.2
Ytilt	arcsec	0.36	83.9	0.11	25.2	63.9	0.07	16.8	42.6
Ztilt	arcsec	0.36	22.0	0.36	22.0	55.9	0.18	11.0	27.9
RSS (microns)					54.4	138.3		31.4	79.6
RSS (arc sec)					0.055	0.141		0.032	0.081

8.5.5   Conclusion

The conjugated primary and secondary mirror segments of GMT allow wavefront errors caused by displacement of the primary segments to be corrected by moving the corresponding secondary segments for the expected full range of misalignment. The residual wavefront errors are negligible over the full field of view for the seeing-limited regime and easily correctable with the deformable secondary mirror for narrow-field adaptive optics.

8.6   Mirror figure control

Wavefront errors that remain after active correction of the optical misalignment terms are addressed with active figure control on the primary and adaptive secondary mirrors. Surface figure corrections on the primary mirror segments are achieved by applying pre-determined force patterns to the back of the mirror to produce the set of natural bending modes. The residual wavefront errors are analyzed in this basis set to arrive at the force values. As previously mentioned only a limited number of modes (20-30) are used due to the inherent stiffness of the mirrors. The forces required to achieve a given level of wavefront correction generally increase as the mode order increases. Ultimately the maximum degree of correction is limited by (a) the amount of force that can be safely applied by the actuators and (b) cross talk between high and low order modes due to force errors in the supports. The control mechanisms and the degree of possible correction are discussed in Chapter 10.

In contrast, the adaptive secondary mirror controller commands displacements of the front surface directly based on sensors that measure the gap between the face sheet and the reference body. The secondary mirror can correct higher order modes than the primary limited by the voice coil actuator power and spacing. The operation of the adaptive secondary mirror is described in Chapter 11.

8.7   Control hierarchy

There is a certain indeterminacy to the process of assigning corrections to different components of the active and adaptive control systems. Field-independent coma, for example, can be

produced by either mirror misalignment or by a figure error. In general, such errors on the current generation Magellan telescopes are corrected by an alignment adjustment. GMT will have two sets of surfaces with figure control with the active primary and adaptive secondary mirrors. The control hierarchy will be addressed through simulations in the next phase of development. We present here some reasonable schemes for distributing the corrections to systems with very different bandwidths, while keeping all actuator travels within comfortable ranges.

In adaptive optics mode, control of wavefront error is by a cascade of systems, from those with the fastest actuators of limited stroke to those with the slowest actuators of longest range. When one set of actuators approaches the limit of its range, certain modes of the accumulated error will be off-loaded to the next system in the chain, effectively implementing a series of low-pass filters of progressively lower cutoff frequency. Details of the spatial and temporal cutoffs will be worked out in the next phase of the project. Table 8-6 gives a preliminary summary of the scheme and identifies the sequence of systems in the cascade.

Table 8-6. A preliminary sequence of systems used to control progressively larger amplitude wavefront errors in adaptive optics mode, with order-of-magnitude update rates.

System	Update rate	Modes corrected
ASM voice coil actuators	up to 2 kHz	All
Secondary segment fine-positioning actuators	1 Hz	Segment tip-tilt, focus, centration
Mount	1 Hz	Telescope pointing
Primary mirror figure	0.03 Hz	First 20 modes of each segment
Secondary hexapod coarse adjustment actuators	0.03 Hz	Secondary tip-tilt, focus, centration
Primary segment positioners	0.001 Hz	Segment tip-tilt, focus, lateral position

A similar progression of control has been successfully implemented at the MMT. Tilt, focus, and coma that build up while the AO is in closed loop over periods of 10-100 s are offloaded to the mount and the secondary hexapod, respectively. The AO loop remains locked during the off-loads, which happen sufficiently slowly that the AO controller has no trouble tracking the changes as they occur.

A different control hierarchy would apply in fast-tracking mode, as shown in Table 8-7. The deformable mirror is not present, and the secondary segments' fine-positioning actuators work over a larger bandwidth to correct for windshake and atmospheric tip-tilt over subapertures.

Table 8-7 . A preliminary control sequence for fast-tracking mode, with order-of-magnitude update rates.

System	Update rate	Modes corrected
Secondary segment fine-positioning actuators	50 Hz	Segment tip-tilt, focus, centration
Mount	1 Hz	Telescope pointing
Primary mirror figure	0.03 Hz	First 20 modes of each segment
Secondary hexapod coarse adjustment actuators	0.03 Hz	Secondary tip-tilt, focus, centration
Primary segment positioners	0.001 Hz	Segment tip-tilt, focus, lateral position

8.8 Cross-talk

The secondary mirror segments are sized to match the beams from the primary mirror segments for on-axis point sources (zero field of view). As the field angle increases, the beams from the primary move off their conjugated secondary segments and eventually illuminate adjacent segments.   Secondary mirror tilt and translation corrections appropriate for one subaperture will not be appropriate for the neighboring segments and ghost images will be formed.

Figure 8-7 is a synthetic interferogram computed for a field radius of 12′ showing illumination across the pupil. The fringes are a characteristic of the (off-axis) wavefront errors of the design. The cross-talk appears as thin arcs between the circular subapertures. They disappear for field angles less than about 10′. For most observations this spill-over effect will be negligible, but for critical applications it can be eliminated by masking off thin chords in the areas of closest approach between segments.
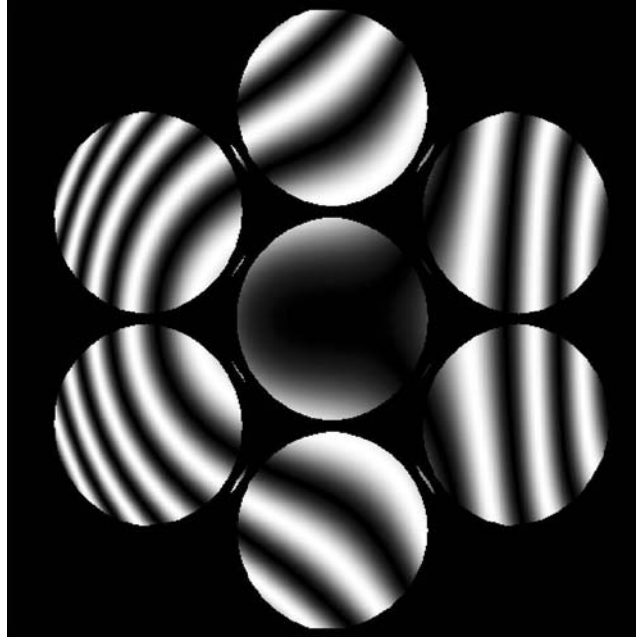
Figure 8-7. Cross-talk between subapertures at a field radius of 12′.

8.9   References

Chanan, G., Mast, T., Nelson, J., Cohen, R., and Wizinowich, P. 1994, in SPIE Conf. Ser. 2199, Advanced Technology Optical Telescopes V, ed. L. M. Stepp, (Bellingham: SPIE), 622

Johns, M. 2005, GMT Optical Alignment I, Document 1297, GMT.

Johns, M. 2005b, GMT Active Optics Wavefront Sensor, Document 1339, GMT.

Schechter, P., Burley, G., Hull, C., Johns, M., Martin, H. M., Schaller, S., Shectman, S., West, S. 2003 in SPIE Conf. Ser. 4837, Large Ground-based Telescopes, ed. J. M. Oschmann, L. M. Stepp, (Bellingham: SPIE), 619